



Coupled chemo-mechanical behavior of CO₂ mineral trapping in the reservoir sandstones during CO₂-EWR

Hong Zheng¹ · Xia-Ting Feng² · Shaojun Li¹ · Shili Qiu¹ · Bin Wang¹

Received: 19 March 2019 / Accepted: 6 July 2019 / Published online: 30 July 2019
© Springer-Verlag GmbH Germany, part of Springer Nature 2019

Abstract

Carbon dioxide (CO₂) sequestration in deep saline aquifers is regarded as a potentially useful method of storing CO₂ due to their large storage capacity. CO₂-trapping mechanisms in such aquifers include solubility trapping, hydrodynamic trapping, structural trapping, and mineral trapping. CO₂-water-rock interactions occurring in saline aquifers injected with CO₂ are known to play a vital role in these trapping mechanisms. Stress is known to have a significant and positive effect on mineral dissolution, and therefore, pressure solution as a coupled chemo-mechanical behavior could make an important contribution to mineral trapping. Geological storage of CO₂ can also be combined with enhanced water recovery (EWR) from deep saline aquifers, a process referred to as CO₂-EWR. By exploiting the fluid during CO₂-EWR, the pore pressure in the reservoir is altered, which could enhance pressure solution between the mineral grains in the reservoir. In this work, the role played by pore pressure in CO₂ mineral trapping from the perspective of pressure solution as a chemo-mechanical coupling process is investigated. To achieve this, seepage-creep tests were performed on sandstone specimens by passing CO₂-NaCl solutions through them at different pore pressures. Experimental results show that the lower the pore pressure a specimen is subjected to, the greater the amount of carbon trapped in the sandstone. On the basis of this result, a geometrical model is established for pressure solution in the materials used that quantitatively describes the mechanism responsible for pressure solution. Geometrical model is then used to analyze the effects of the various factors affecting the role played by pressure solution in CO₂ mineralization sequestration (mineral type, pore pressure, porosity, and particle size). The results of the analysis are particularly instructive for the evaluation of long-term CO₂ storage in terms of pressure solution. As for CO₂-EWR, apart from relieving pressure buildup, increasing CO₂ injection, regulating CO₂ migration, and restricting CO₂ leakage, it also enjoys the advantage of enhancing mineral trapping.

Keywords CO₂ mineralization sequestration · Pressure solution · Pore pressure · Seepage-creep test · Geometrical model

Introduction

During CO₂ sequestration in deep saline aquifers, CO₂ that is dissolved and compressed in the saline reservoir and free phase aggregating along the bottom of the caprock (Lemieux 2011) may cause a considerable buildup of pressure in the storage formation and displacement of the native brine

(Myrntinen et al. 2012; Birkholzer et al. 2009). Increasing the pressure in the storage formation in this way may induce the overlying caprock to fracture or activate faults, which could, in turn, trigger the leakage of CO₂.

For injection-only, industrial-scale, saline-formation geologic CO₂ storage, pressure buildup can limit CO₂ storage capacity and security. Moreover, water demand and parasitic energy costs associated with CO₂ capture and storage operations are large. CO₂ geological storage combining with deep saline water recovery (CO₂-EWR) as a new CO₂ capture, utilization and storage technology which not only achieves deep emission reduction, but also alleviates the water shortage situation by exploiting the fluid from CO₂ storage formation (Davidson et al. 2009; Kobos et al. 2011; Aines et al. 2011; Randolph and Saar 2011).

✉ Hong Zheng
zhengh@whrsm.ac.cn

¹ State Key Laboratory for Geomechanics and Geotechnical Engineering, Institute of Rock and Soil Mechanics, Chinese Academy of Sciences, Wuhan 430071, China

² Key Laboratory of Ministry of Education on Safe Mining of Deep Metal Mines, Northeastern University, Shenyang 110819, China

Brine production in CO₂-EWR may enable the development of utilization in terms of freshwater production, saline cooling water for power plants, geothermal power, and make-up water for oil, gas, and geothermal energy production (Bachu 2016; Hunter et al. 2017; Buscheck et al. 2017; Niu et al. 2017). In addition, these brine-utilization options help improve the economic feasibility of CO₂ capture and storage. Moreover, the combined process obviously provide an opportunity to relieve pressure buildup, increase CO₂ injectivity, regulates CO₂ migration, and restricts CO₂ leakage (Buscheck et al. 2012; Birkholzer et al. 2012). All these effects are beneficial to the secure and efficient trapping of CO₂ in deep saline aquifers.

Bachu and Adams (2003) proposed four trapping mechanisms in CO₂ sequestration in deep saline aquifers: solubility trapping, hydrodynamic trapping, structural trapping, and mineral trapping. Since CO₂ could be permanently stored in the lithosphere in a solid phase (e.g., calcite, dolomite, magnesite, siderite, or dawsonite), mineral trapping has been studied as the most effective long-term storage process for the CO₂ injected into saline aquifers by many scholars (Palandri et al. 2005; Regnault et al. 2005; De Silva et al. 2015). However, CO₂ sequestration in saline aquifers has been investigated for only a couple of decades, and very few chemo-thermo-mechanical studies have focused on mineral trapping. From the point of view of mineralization in saline aquifers, CO₂ becomes trapped as a result of chemo-mechanical coupling (Labus et al. 2016; Ghafoori et al. 2017). Pressure solution as a chemo-mechanical coupling process is driven by the gradient in the chemical potential between the highly-stressed contact junctions and less-stressed sites on the pore walls (Yasuhara et al. 2011; Bond et al. 2016; Jiang et al. 2019). In CO₂ sequestration, high stress enhances the CO₂-water-rock interactions. Therefore, relieving pore pressure buildup in CO₂-EWR has a beneficial effect on mineral trapping.

CO₂ mineral trapping achieves the carbon fixation in lithosphere by means of certain chemical reactions occurring between the rock in the reservoir and CO₂-rich brine. Many researchers (Gunter et al. 2004; Aagaard et al. 2004; Carroll and Knauss 2005; Pokrovsky et al. 2009; Hangx and Spiers 2009; Liteanu et al. 2012) have investigated the CO₂-water-rock system in the context of CO₂ trapping. Chemical reactions involved generally relate to two kinds of mineral: (1) relatively fast-reacting minerals, e.g., carbonates, which are present in either the framework grains or intergranular cement and (2) Ca-, Mg-, or Fe-rich framework minerals, e.g., feldspars, clays, micas, and iron oxides, which slowly mineralize with CO₂ via slow, long-term, reactions. Carbonates dissolve relatively rapidly in the underground water and react with the CO₂ forming bicarbonate ions. On the other hand, the Ca-, Mg-, or Fe-rich detrital rock reacts with CO₂-rich brine to generate carbonate minerals.

Compared to the former, the latter process is a more stable and superior way of realizing mineral trapping in reservoirs. However, the effect of chemo-mechanical coupling on mineral trapping in the form of pressure solution has not been considered in the previous studies.

To investigate the effect chemo-mechanical coupling as on CO₂ mineralization sequestration, experiments were performed using specimens made of quartz-feldspar-detrital sandstone. The use of storage reservoirs made from such material is a more stable and superior approach to mineral trapping in reservoirs compared to using carbonates. As pressure solution is directly influenced by pore pressure, the contribution that pressure solution makes to mineral trapping can be promoted by depressing the reservoir during CO₂-EWR. To investigate the role played by pore pressure in carbon fixation, tests were carried out using different pore pressures. A physical model is also developed to quantitatively describe the mechanism responsible for chemo-mechanical coupling in CO₂ mineralization sequestration. Effect factors of chemo-mechanical coupling in CO₂ mineralization sequestration (mineral type, pore pressure, porosity, and mineral particle size) were then investigated using the geometrical model to perform numerical calculations.

Experiments and results

Seepage-creep tests were first conducted to reveal the effect of pore pressure on the mechanical properties and mineral trapping ability of reservoir rock samples. In the present work, the pore fluid was simplified to a mixture of sodium chloride (NaCl) solution and CO₂. The saline solution prepared had NaCl concentration of 0.1 mol/L and all experiments were performed at 25 °C.

A confining pressure of 20 MPa was used in the triaxial compression tests. A deviatoric stress of 10 MPa and differential hydraulic pressures of 1, 3, and 5 MPa was used in the seepage-creep tests. In addition, the porosity distribution and degree of carbon fixation were investigated via a series of micro-tests, including scanning electron microscopy (SEM) and mercury intrusion porosimetry (MIP).

Mineral composition and pore structure

Sandstone used in the experiments was mainly composed of quartz and feldspar cemented by hydromica and clay minerals. More precisely, quartz occupied 55% of the total mass, while other 45% was made of feldspar (potash feldspar, sodium feldspar, and calcium feldspar in the ratios 4:1:1, respectively).

SEM was used to observe microstructure (pore structure) and contact shape between the mineral particles in sandstone. Figure 1a, b shows micrographs of the sandstone

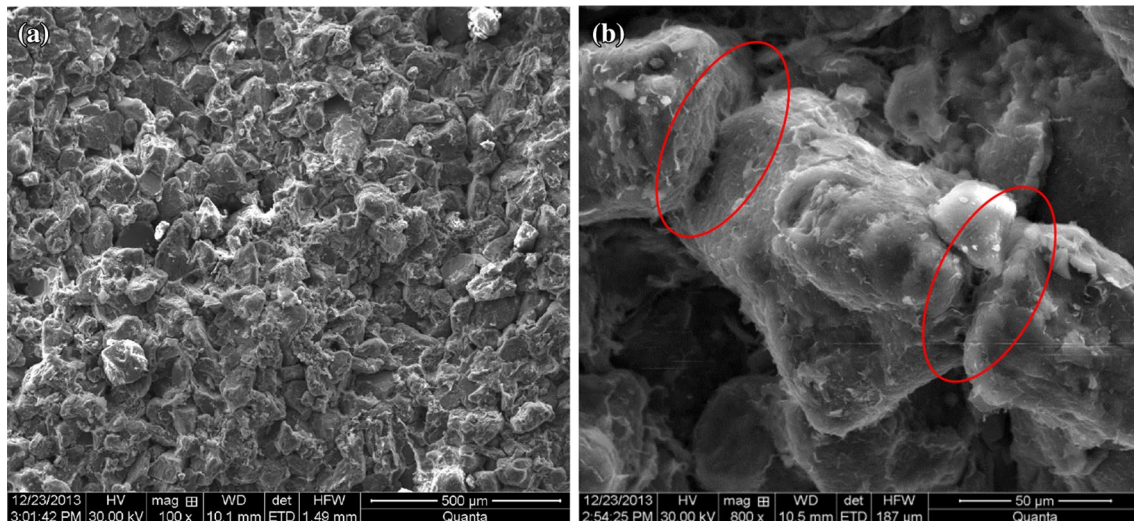


Fig. 1 SEM images of the sandstone recorded using magnifications of: **a** $\times 100$, and **b** $\times 800$

recorded at magnifications of $100\times$ and $800\times$, respectively. In addition, the sizes of the mineral particles ranged from 0.002 to 0.35 mm and the contact faces between adjacent particles could be readily observed, as shown in Fig. 1b.

Laboratory experimentation

A serial of laboratory tests were then carried out using sandstone specimens to investigate the effect of pore pressure on the deformation, pore structure characteristic, and mineral trapping ability of the sandstone reservoirs.

Seepage–creep tests and results

Three seepage–creep tests were performed corresponding to three different pore pressures. Flow-through solution used in each case was 0.1 mol/L NaCl solution saturated with CO_2 (at a temperature of 25°C and pressure of 1 MPa).

As shown in Fig. 2, other constant conditions used in the three tests are a confining pressure of 10 MPa, axial deviatoric stress of 5 MPa, and a temperature of 25°C . Meanwhile, the three tests varied in the differential hydraulic pressures that were of applied (1, 3, and 5 MPa, respectively). To be more precise, the specimens in the triaxial testing apparatus were subjected to inlet pressures of 2, 4, and 6 MPa, respectively, while the outlet pressure was kept at 1 MPa (as the NaCl solution was saturated with CO_2 at a pressure of 1 MPa).

Result in Fig. 3 shows axial creep curves produced using three differential hydraulic pressures. In Fig. 3, the axial strain clearly increases, as the pore pressure is reduced. The three curves each increase at first (at the beginning of the tests) and then gradually enter stable phases.

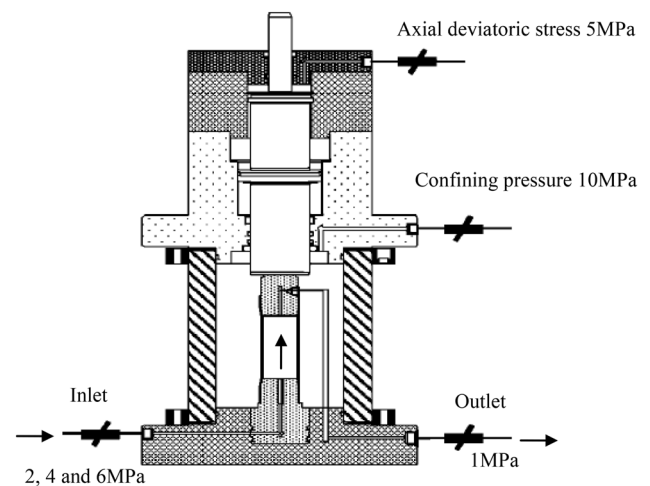


Fig. 2 Pressure conditions applied to the sandstone specimens in the triaxial testing apparatus

MIP tests and results

Before and after the seepage–creep tests, MIP was applied to comparative investigate the pore size distribution of initial sample and the samples subjected to different pore pressures. In Fig. 4, the x coordinate represents the logarithm of the pore size and the y coordinate represents the pore volume accumulation ratio expressed as a percentage. In addition, the upward deflection of a curve reflects concentration of the pore size. As can be seen from the diagram, logarithmic pore size of initial sample is approximately centered between 3.9 and 4.1. Result shows that decreasing pore pressure leads to an increase in the number of sections, where uprush occurs in the curve. At the same time, the logarithmic pore size at

Fig. 3 Axial creep curves produced using specimens subjected to differential hydraulic pressures of 1, 3, and 5 MPa

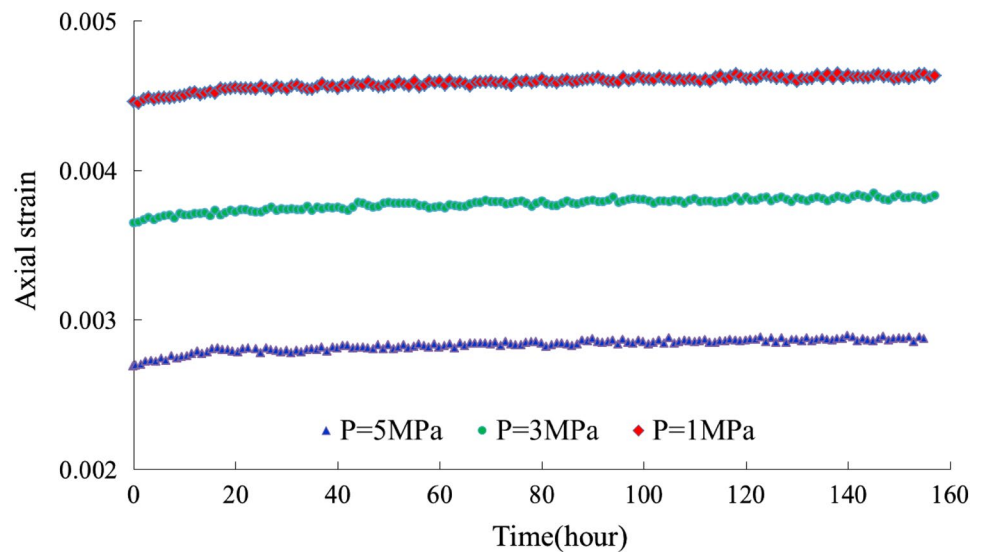
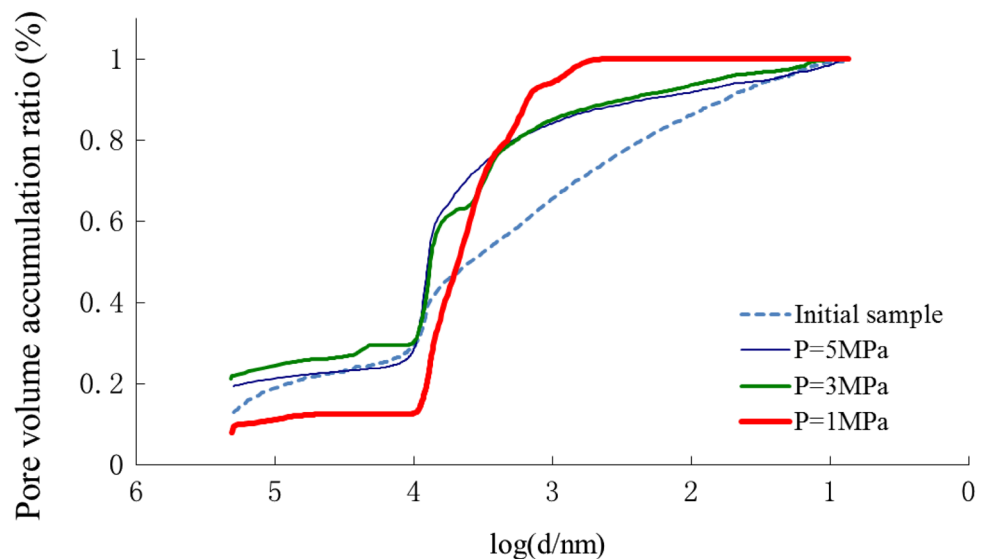


Fig. 4 Pore size distribution curves (in differential form) for initial sample and specimens subjected to three different pore pressures



which uprush occurs decreases. This means that the value at which pore size is concentrated should increase as pore pressure is enlarged, i.e., pore space expanded with the increasing pore pressure. From the point of view of poromechanics (Coussy 2004), pore deformation is effected by stress field, pore pressure, and compressibility of porous material and pore fluid. Porosity is the ratio of the pore space in the rock to the bulk volume of the rock. Therefore, the result in Fig. 4 reflects porosity and pore pressure as positive correlation in given conditions.

SEM tests and results

To assess the effect of pore pressure on the degree of carbon fixation occurring in the reservoir, three specimens were sampled at the same location used for the SEM tests.

These samples were subjected to quantitative analysis—the results (full-scan mass spectra) are shown in Table 1. As can be seen from these results, the higher the pore pressure the specimen is subjected to, the smaller the amount of carbon found in the sandstone after creep testing using CO_2 -NaCl solution.

Methods

Theoretical foundation of methodology

CO_2 injection into saline groundwater changes the chemical environment in the reservoir. These changes give rise to a series of reactions between the pore fluid and rock matrix as chemo-mechanical coupling process. From the point

Table 1 Quantitative analysis results (full-scan mass spectra) for sandstone subjected to CO₂-NaCl flow-through using solutions with differential hydraulic pressures (*P* = 1, 3, and 5 MPa)

P (MPa)	C (%)	O (%)	Na (%)	Mg (%)	Al (%)	Si (%)	K (%)	Ca (%)	Fe (%)	Pd (%)	Au (%)
1	20.03	51.53	0.39	0.57	1.10	15.56	0.32	1.31	1.56	1.78	5.85
3	16.16	52.01	1.71	0.58	1.15	14.56	0.42	1.48	0.64	1.81	9.48
5	6.25	48.54	0.89	1.27	6.25	22.92	1.56	1.18	2.94	1.35	6.85

of view of the chemo-mechanical coupling mechanism in CO₂ sequestration in deep saline aquifers, pressure solution (which depends on the disjoining pressure) (Heidug 1995) plays a significant role in mineral trapping in high stress situations like those found in deeply buried reservoirs.

The stress on the contact face between adjacent particles is given by

$$\sigma_{\text{contact}} = \sigma' / R_C, \tag{1}$$

where $\sigma' = \sigma - bp$ is the effective stress with σ the total stress, p is the pore pressure, and b is the Biot coefficient given by $b = 1 - R_C$, where R_C is the contact area ratio, that is, the ratio of the contact area, A_C , to the total area, A . The disjoining pressure is the driving force causing pressure solution and is given by

$$\sigma_a = \sigma_{\text{contact}} - p = \frac{\sigma - p}{R_C}. \tag{2}$$

In high stress regions, the mineral surface is subjected to pressure solution. The dissolved minerals then diffuse into the pore space (low stress) in the water film between contact areas. As pressure solution progresses, the contact area increases, so that σ_a decreases. Eventually, equilibrium is reached, wherein pressure solution is no longer thermodynamically favorable. This equilibrium stress is approximately given by (Stephenson et al. 1992)

$$\sigma_c = \frac{E_m(1 - T/T_m)}{4V_m}, \tag{3}$$

where E_m is the heat of fusion, T_m is the temperature of fusion, V_m is the molar volume, and T is the temperature. The dissolution rate associated with pressure solution is given by (Taron and Elsworth 2010)

$$m_{\text{diss}}^{\text{PS}} \text{ (mol/s)} = k^+ A_{\text{rx}} \frac{\Delta\mu}{RT} = \frac{k^+ A_{\text{rx}} V_m (\sigma_a - \sigma_c)}{RT}, \tag{4}$$

where k^+ is the dissolution rate constant, A_{rx} is the reactive area, and R is the gas constant. As compaction from pressure solution progresses, σ_a decreases, as the area of contact increases. In addition, the dissolution rate gradually falls and eventually terminates when σ_a is equal to the equilibrium stress σ_c .

If the stress condition changes, e.g., the formation stress σ increases or pore pressure p decreases, then pressure solution restarts. When this is exploited to accomplish CO₂ storage by pressure solution, the pore pressure needs to be decreased, as this will enlarge the disjoining pressure and enhance the dissolution rate, thus facilitating mineral trapping of the CO₂.

Three-dimensional chemo-mechanical coupling model

A number of geometrical models have been developed for pressure solution as a coupling chemo-mechanical behavior and used to investigate the effect of dissolution on strain/stress and permeability (Liu et al. 2006; Pietruszczak et al. 2006). To quantitatively describe CO₂ mineralization sequestration in the context of porous media theory, a geometrical model is established for chemo-mechanical coupling. Considering that the saline aquifer is composed of rock matrix and pore fluid (CO₂ or/and brine), representative volume element (RVE) involves mineral particle and porous space filled by fluid. On the basis of SEM results shown in Fig. 1b, the shape of mineral particle was simplified as spheroidal particle in RVE.

Geometrical model subjected to three-dimensional stress field is shown in Fig. 5. The spherical element in the diagram is subject to contact via the six faces shared with its six adjacent spherical elements, which lie in the directions of the three major principal stresses. In Fig. 5a, the part of the sphere inside the cube represents the mineral particle, and the rest of the space inside the cube (but outside the sphere) represents the pore volume. The initial area of contact is taken to be A_c^0 , the radius of the sphere is r , and the height of the top part of the sphere that is outside the cube is d_0 . Thus, the length of the side of the cube is $2(r - d_0)$.

Using the geometrical model shown in Fig. 5, mathematical expressions for the volume of the sphere top $V_d^{(t)}$, the contact area $A_c^{(t)}$, and the total area $A^{(t)}$ at any given time t were established as

$$V_d^{(t)} = \left(rd^{(t)2} - \frac{1}{3}d^{(t)3} \right) \pi \tag{5}$$

$$A_c^{(t)} = \left(2rd^{(t)} - d^{(t)2} \right) \pi \tag{6}$$

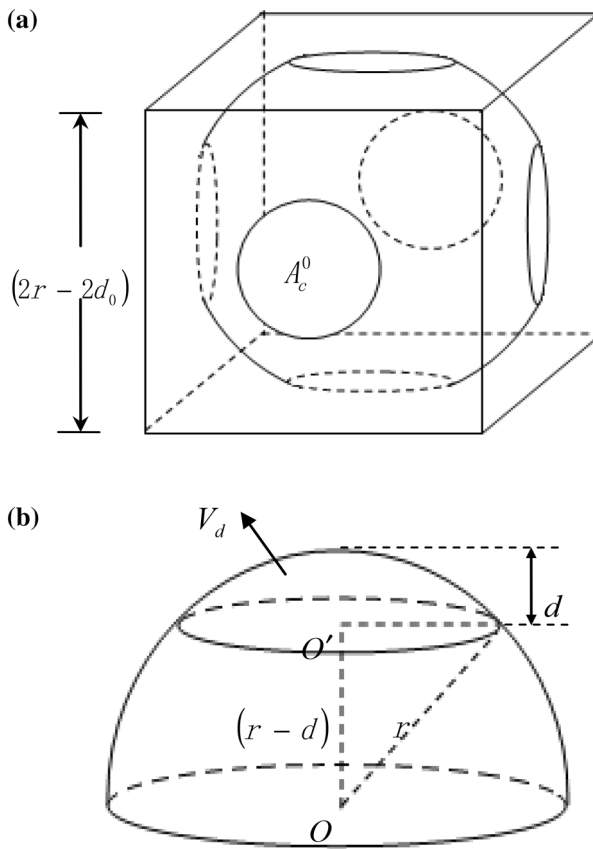


Fig. 5 RVE of the geometrical model used for chemo-mechanical coupling

$$A^{(t)} = 4(r - d^{(t)})^2, \tag{7}$$

where $d^{(t)}$ is the height of the top part of the sphere at time t . The initial volume of the sphere top is $V_d^0 = (rd_0^2 - d_0^3/3)\pi$, the initial contact area is $A_c^0 = (2rd_0 - d_0^2)\pi$, and the total initial area is $A^0 = 4(r - d_0)^2$.

As chemo-mechanical coupling proceeds, the mineral particles become compacted increasing V_d , d , and A_c . The rate of increase in V_d is the dissolution volume rate of the mineral particle, which can be deduced from Eq. (4) to be

$$\dot{V}_d = \frac{k^+ A_{rx} V_m V_m^d (\sigma_a - \sigma_c)}{2RT}, \tag{8}$$

where V_m^d is the dissolution volume per mole. For a congruent dissolution mineral, V_m^d is equal to the molar volume; for an incongruent dissolution mineral, V_m^d is less than the molar volume.

As the disjoining pressure is equal to the amount by which the pressure acting at a contact area exceeds the hydrostatic pore pressure, increasing the formation pressure or decreasing the pore pressure would both accelerate

the chemo-mechanical coupling process. Furthermore, regardless of the orientation of the principal stress axis, the pressure solution equations need to be calculated using the three principal stresses in the three-dimensional stress field. The relational expression is

$$\dot{V}_{dij} = \frac{k^+ V_m V_m^d}{2RT} \begin{bmatrix} (\sigma_{a1} - \sigma_c) A_{rx1} & 0 & 0 \\ 0 & (\sigma_{a2} - \sigma_c) A_{rx2} & 0 \\ 0 & 0 & (\sigma_{a3} - \sigma_c) A_{rx3} \end{bmatrix}, \tag{9}$$

where σ_{a1} , σ_{a2} , σ_{a3} are the three principal stresses and A_{rx1} , A_{rx2} , A_{rx3} are the three pairs of reactive areas.

Numerical calculations

From the point of view of chemo-mechanical coupling behavior, the extent of CO₂ mineral trapping in saline aquifers is related to the pressure solution rate and chemical reaction duration. Clearly, the faster the pressure solution rate and the longer the duration of the chemical reaction, the greater the amount of CO₂ involved in mineral trapping. In CO₂-EWR, the dissolution rate of the mineral particles will change along with the underground water pressure during the CO₂ injection and brine exploitation. In addition, as dissolution proceeds, the area of the contact face gradually increases as a result of interparticle dissolution and compaction. Thus, the disjoining pressure (which is the driving force responsible for pressure solution) is affected by the contact area and pore pressure.

The duration of the chemical reactions involved in CO₂ mineral trapping depends on the rate at which the disjoining pressure approaches the equilibrium stress. Therefore, the relationships between and evolution of the particle contact area, pore pressure, and pressure solution rate all play an important role in determining the complicated way in which pressure solution varies during CO₂ mineral trapping. The basic expressions for the model are given in Eqs. (2)–(8), and these allow the amount of CO₂ captured via mineral trapping to be quantitatively evaluated using a method of iteration.

In this work, three assumptions are made.

- Pure mechanical compaction, without pressure solution, does not make a significant contribution to the contact area between adjacent particles. Thus, the effect of mechanical deformation on the area of the contact face is neglected.
- A fully process of pressure solution refers to the serial dissolution–diffusion–precipitation system. However, diffusion at contacts and precipitation at unstressed sites in porous media are controlled by concentration gradient and make no contribution to chemo-mechanical coupling.

Therefore, the effect of diffusion at contacts and precipitation at unstressed sites is neglected.

- In this geometrical model, only the primary mineral involved in CO₂ mineral trapping is considered. That is, any contributions made by secondary minerals are ignored.

The mineral composition of the reservoir rock influences the type of chemical reaction that occurs with CO₂. In addition, the size of the mineral particles and cementation structure in the saline aquifer determine the porosity and permeability of the reservoir. In other words, both mineral composition and rock structure play important roles in the CO₂ trapping process. For a given reservoir, the mineral composition and particle size will be fixed. Then, the contribution made by pressure solution to CO₂ trapping will depend on the change in pore pressure during CO₂-EWR. For our chemo-mechanical coupling model, an appropriate value for d_0 can be derived from the porosity ϕ_0 and mineral particle radius r determined from the MIP and SEM results. These parameters are related via the expression:

$$\phi_0 = 1 - \frac{\left[\frac{4}{3}\pi r^3 - 6\pi \left(rd_0^2 - \frac{1}{3}d_0^3 \right) \right]}{(2r - 2d_0)^3} \tag{10}$$

Based on the initial geometric dimensions used in the geometrical chemo-mechanical coupling model for pressure solution and change in pore pressure, the quantity of mineral undergoing dissolution at each time step can be calculated by iteratively applying the relationships given above via the loop, as shown in Fig. 6.

The loop in Fig. 6 involves three steps: (1) calculate the dissolution volume in the time step using Eq. (8); (2) calculate the current contact area A_c and current total area A at the end of the time step using Eqs. (5)–(7); and (3) update the disjoining pressure σ_a using Eq. (2) and compare it with the equilibrium stress σ_c . If $\sigma_a > \sigma_c$, the loop continues; otherwise, the whole loop terminates.

Factors affecting results and discussion

According to the chemo-mechanical coupling mechanism underlying pressure solution, the reaction course is controlled by the disjoining pressure, temperature, dissolution rate constant, and reactive area. In this section, the geometrical chemo-mechanical coupling model for pressure solution is used to investigate the effect of various factors affecting the role played by pressure solution in CO₂ mineralization sequestration (namely, the mineral involved, pore pressure, particle size, and porosity).

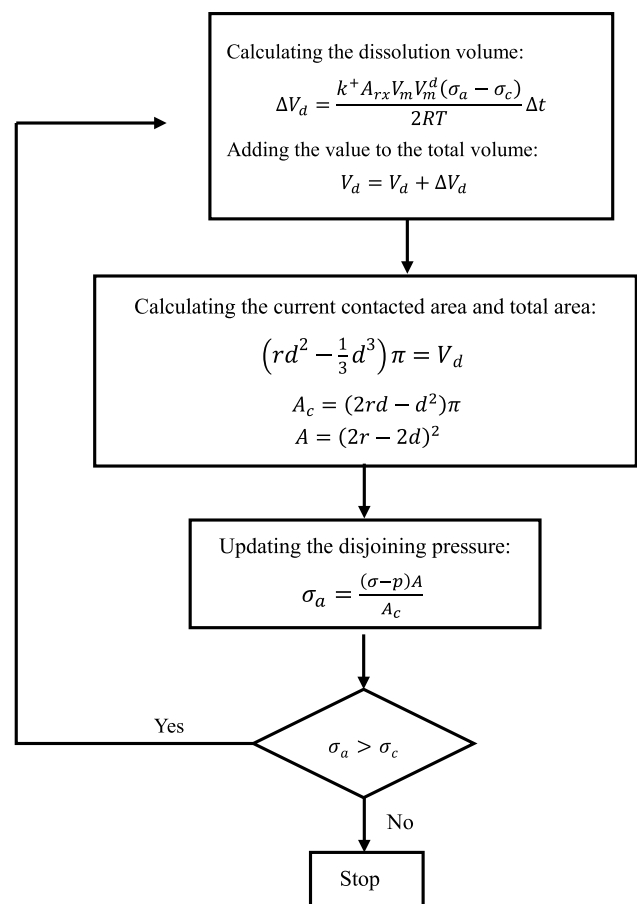
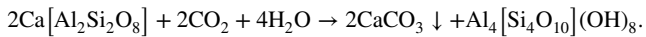
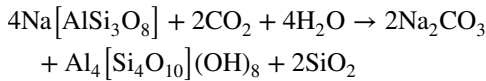
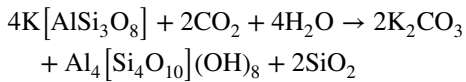


Fig. 6 Flow chart showing the steps involved in the iterative loop used to numerically calculate the pressure solution

Effect of different minerals

The sandstone used in the experiments mainly consists of quartz, potash feldspar, sodium feldspar, and calcium feldspar. To further investigate the effect of different minerals on mineral trapping, the chemical reactions that the different minerals undergo with CO₂-rich brine first need to be determined.

When a seepage-creep test is carried out using a flow-through of CO₂-NaCl solution, it is the quartz and feldspar in the sandstone that mostly undergo chemical dissolution and reaction due to the combined effect of the acidic fluid and stress field. Quartz, as one of the main minerals present in sandstone, is only part-dissolved and does not participate in the reaction with the CO₂-NaCl solution. However, the other main mineral, feldspar (in the form of potash feldspar, sodium feldspar, and calcium feldspar) will react with the dissolved CO₂ and generate kaolinite and quartz as follows:



Thus, the injected CO_2 could be present in dissolved form in the pore fluid, but it may also be precipitated out by calcium ions (and other ions that may also be in the pore solution, e.g., magnesium ions and ferrous ions that are in sandstone). In this way, CO_2 is absorbed in the form of both soluble and insoluble carbonates.

The dissolution rates of different minerals are likely to be very different, and for a given mineral, the dissolution rate will also vary with the temperature of the environment. Therefore, in this section, the dissolution rates of potash feldspar, sodium feldspar, and calcium feldspar are considered at two temperatures (20 and 90 °C) to give sufficient contrast in the analysis. As can be seen from Fig. 6, for a given mineral, some of the parameters in the formulae used are constant (including heat of fusion E_m , temperature of fusion T_m , molar volume V_m , gas constant R , and dissolution

volume per mole V_m^d). Moreover, the dissolution rate constant k^+ is related to the temperature T . During the pressure solution calculation, the parameters in Eqs. (5)–(7) are updated in each step.

In this section, the different minerals are subjected to the same three-dimensional in situ stress (30 MPa), and the radii r and heights of the sphere top part outside the cube (d_0) are also taken to be the same for the different minerals. Besides this, the initial pore pressures are taken to be the same (10 MPa) and the pore pressure decreases linearly with time. The values of the parameters that do differ are listed in Table 2.

The initial pore structure is described by the geometry, as shown in Fig. 5. According to the test results in “[Mineral composition and pore structure](#)”, the porosity in this section is assumed to be 40% and the particle diameter is taken to be 0.4 mm. Thus, the initial contact face has an area of $1.32 \times 10^{-2} \text{ mm}^2$. The principal stress condition is set to 30 MPa in each of the three directions and the pore water pressure is set to 10 MPa. Our aim here is to evaluate the amount of CO_2 trapped per cubic meter of rock over a period of 150 months. The cumulative numbers of moles of CO_2 sequestered by pressure solution using potash feldspar, sodium feldspar, and calcium feldspar are shown in Fig. 7 for temperatures of 20 and 90 °C.

Table 2 Parameters used to calculate the pressure solutions of the different feldspars (Ague and Brimhall 1989; Gérard et al. 1997)

Mineral	V_m (m ³ /mol)	V_m^d (m ³ /mol)	k^+ (20 °C) (mol/m ² s)	k^+ (90 °C) (mol/m ² s)	E_m (kJ/mol)	T_m (K)
Sodium feldspar	1.00e−4	1.36e−5	5.14e−13	2.23e−11	59.257	1391
Potash feldspar	1.08e−4	2.92e−5	2.15e−12	4.55e−11	48.609	1473
Calcium feldspar	1.01e−4	1.42e−5	6.66e−10	2.71e−9	81.096	1830

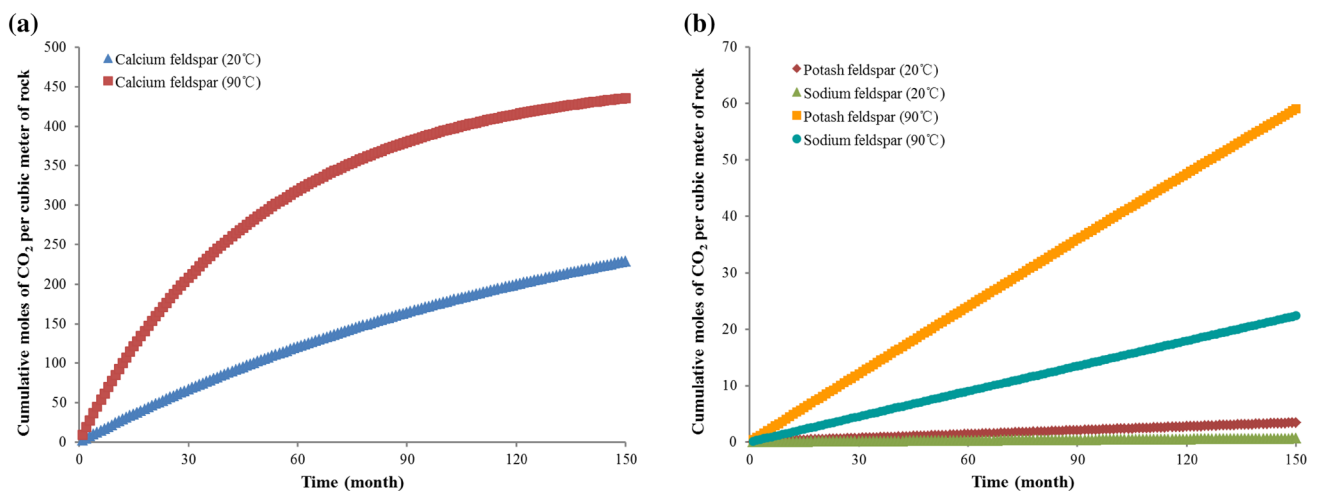


Fig. 7 Cumulative moles of CO_2 per cubic meter of feldspar: **a** potash, **b** sodium and calcium calculated over a 150-month period at temperatures of 20 °C and 90 °C

On comparing the results for the different feldspars in Fig. 7, it is clear that the feldspar with the largest dissolution rate constant (calcium) displays the most significant capacity for carbon fixation. In addition, because of the positive relationship between dissolution rate constant and temperature, higher temperature is beneficial for mineral trapping CO₂ by pressure solution. This temperature advantage is most prominent in the case of calcium feldspar (compared with potash feldspar and sodium feldspar).

Effect of pore pressure

The quantitative analysis results in Table 1 reflect the effect of pore pressure on mineral trapping in the quartz–feldspar–detrital sandstone. The mathematical formulation given in “Three-dimensional chemo-mechanical coupling model” for pressure solution allows us to investigate that the role pore pressure plays in mineral trapping.

The geometrical model established for pressure solution gives a quantitative description of the chemo-mechanical

coupling mechanism involved in CO₂ mineralization sequestration. According to Eqs. (2)–(4), the rate of pressure solution is negatively related to pore pressure. That is, the pressure solution rate decreases when the pore pressure increases. Once the pore pressure increases to the point at which the disjoining pressure is equal to the equilibrium stress in the pressure solution process, mineral trapping by pressure solution ceases (unless the disjoining pressure can be made to exceed the equilibrium value once again). To investigate the effect of pore pressure on pressure solution, the amount of CO₂ sequestered by the different minerals at different pore pressures (2, 6, and 10 MPa) were determined and are compared in Fig. 8. Beside the pore pressure, the initial geometrical parameters of the mineral particles and the principal stress conditions are the same here as in “Effect of different minerals”. In addition, the temperature used was 90 °C in each case.

From Fig. 8a, cumulative moles of CO₂ sequestered by pressure solution per cubic meter of sodium feldspar over 150 months can be seen to increase from 25.6 to 43.9 mol

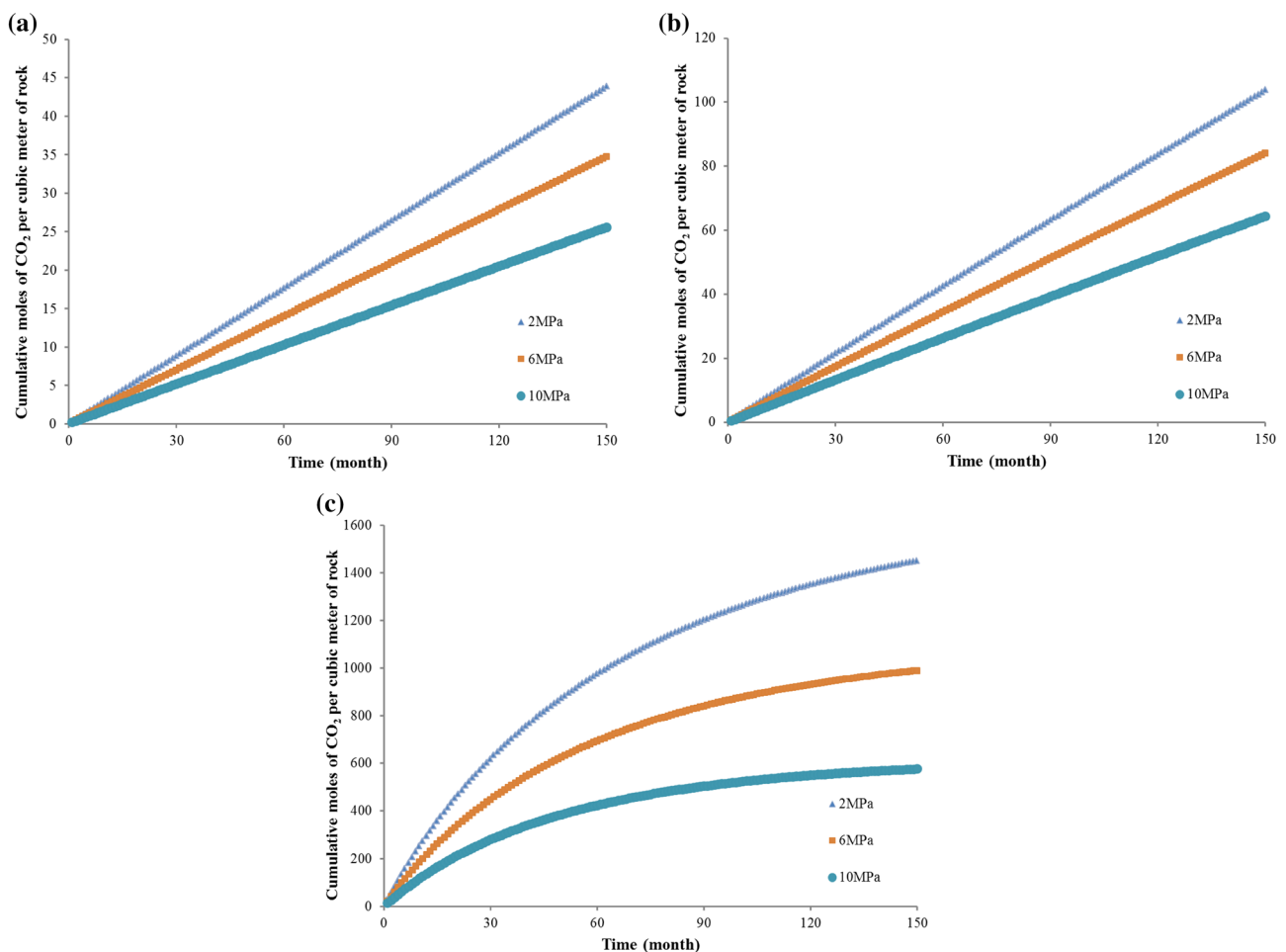


Fig. 8 Cumulative moles of CO₂ per cubic meter of **a** sodium feldspar, **b** potash feldspar, and **c** calcium feldspar for pore pressures of 2, 6, and 10 MPa

when the pore pressure is reduced from 10 to 2 MPa. The corresponding increases for potash and calcium feldspars are from 64.4 to 103.6 mol and 575.7 to 1450.5 mol. Numerical simulation results in Fig. 8 once again proved the conclusion obtained from the previous test results, i.e., reducing pore pressure clearly increases the amount of CO₂ sequestered as a result of pressure solution. In addition, the time taken to reach a targeted amount of CO₂ sequestration via pressure solution can, therefore, be significantly shortened by reducing the pore pressure.

To further investigate the effect of varying pore pressure on pressure solution, the different minerals were compared using pore pressures that were increased on a monthly basis. The temperature was again set to 90 °C and the initial pore pressure was 10 MPa. This was increased at rates of 1, 0.1, and 0.01 MPa/month, giving the results, as shown in Fig. 9. The results show that, as time goes by, pressure solution stops when pore pressure rises to

a certain threshold. That is, cumulative moles of CO₂ sequestered via pressure solution stops growing when the pore pressure reaches the threshold, i.e., when disjoining pressure σ_a is equal to the equilibrium stress σ_c .

Comparing the curves obtained using the three different rates of pore pressure change, it can be seen that the critical pressure increases, as the rate of pore pressure change increases. In the calcium feldspar case, for example, the critical pressures are found to be 11.31, 14.2, and 18 MPa, when the rate of pressure increase is 0.01, 0.1, and 1 MPa/month, respectively.

The results in Fig. 9 show that the rate at which the pore pressure is increased can influence pressure solution in the feldspar. Therefore, controlling the rate at which pore pressure increases is important for the mineral trapping of CO₂ in the reservoir formation. This is especially the case when the pore pressure is high and exceeds the critical pressure, as

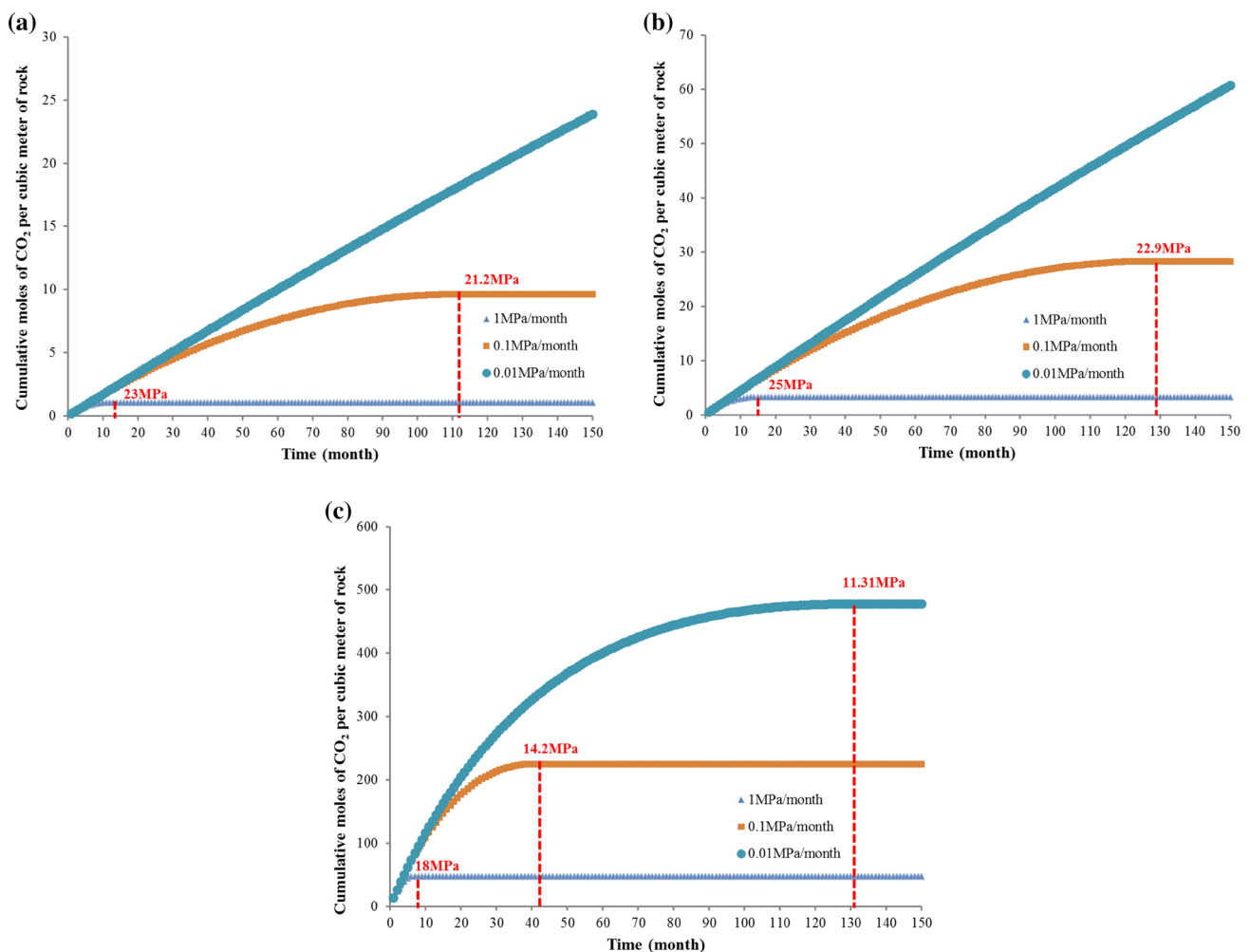


Fig. 9 Cumulative moles of CO₂ per cubic meter of **a** sodium feldspar, **b** potash feldspar, and **c** calcium feldspar when the pore pressure increases at rates of 1, 0.1, and 0.01 MPa/month

reducing the pore pressure is a very effective way of restarting the mineral trapping process via pressure solution.

Effect of porosity and mineral particle size of the reservoir

According to the three-dimensional geometrical model, pressure solution is strongly dependent on the pore structure, i.e., the porosity and particle size. In fact, mineral particle structure is one of the key factors (besides mineral type) affecting the ability of a reservoir to capture CO₂. In this section, the porosity and mineral particle size are analyzed to reveal their influence on CO₂ sequestration via pressure solution.

Results in Fig. 10 show that cumulative moles of CO₂ per cubic meter of feldspar samples with different porosities (45%, 40%, and 35%). In each case, the particle diameters are the same (0.4 mm). Similarly, the amount of CO₂ sequestered using samples with particles of different diameter (0.4, 0.2, and 0.04 mm), but identical porosity (40%) is compared

in Fig. 11. Apart from these differences in porosity and particle size, the other conditions are the same (the principal stress is 30 MPa in all three directions, the pore pressure is constant at 10 MPa, and like in “Effect of pore pressure”, the temperature is 90 °C).

Comparing the curves shown in Fig. 10, it is clear that CO₂ sequestration is accelerated by increasing the porosity of the feldspar. In addition, the positive role played by porosity in calcium feldspar is more significant than it is in the other two feldspars. On the other hand, the data shown in Fig. 11 reveal that the smaller the diameters of the particles involved, the greater the amount of CO₂ sequestered via pressure solution (all other parameters being equal). From this perspective, porosity and particle size are very important factors to consider when mineral trapping is employed for long-term CO₂ storage.

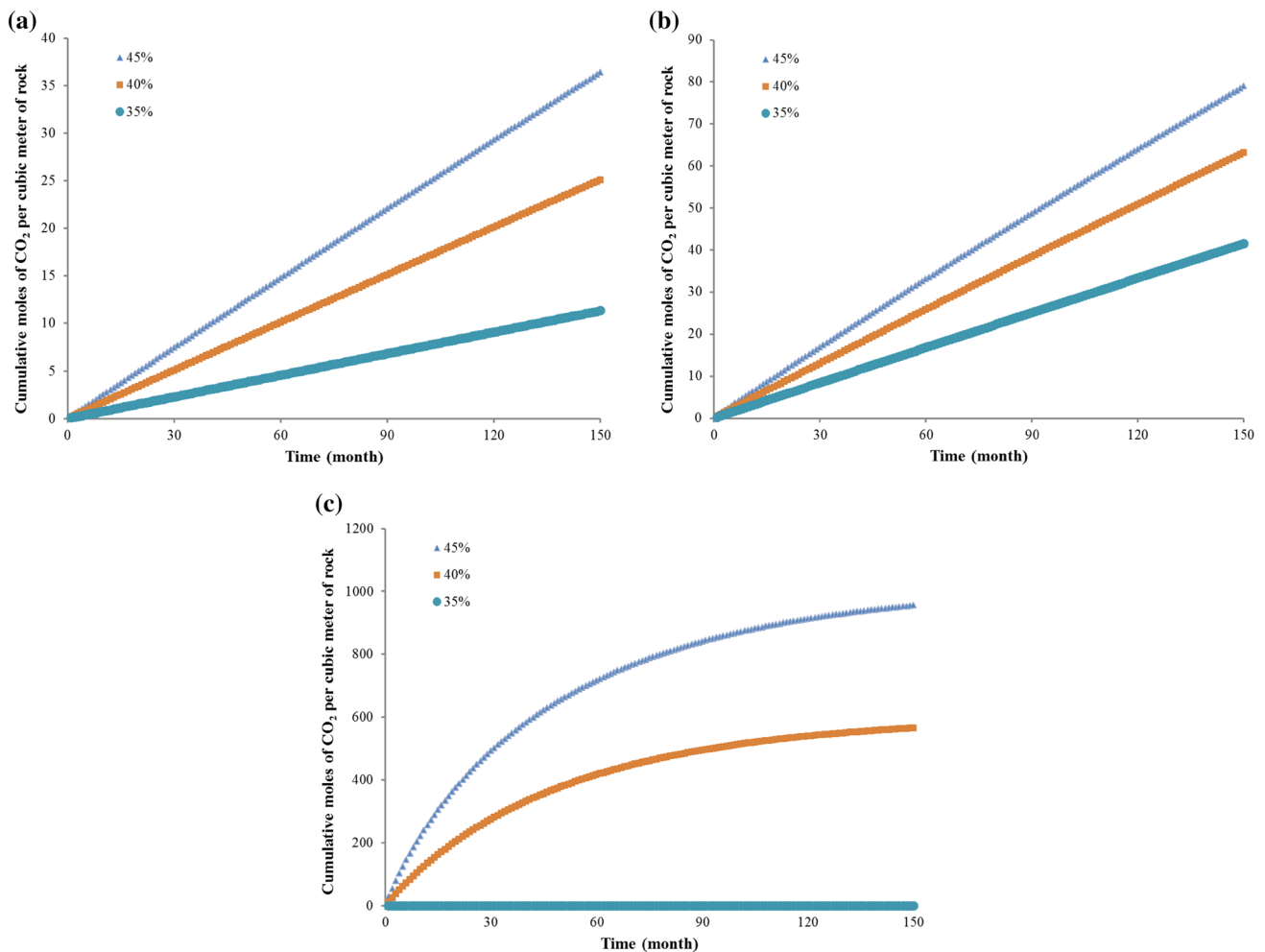


Fig. 10 Cumulative moles of CO₂ per cubic meter of **a** sodium feldspar, **b** potash feldspar, and **c** calcium feldspar for different porosities (45%, 40%, and 35%) but identical particle size (0.4 mm)

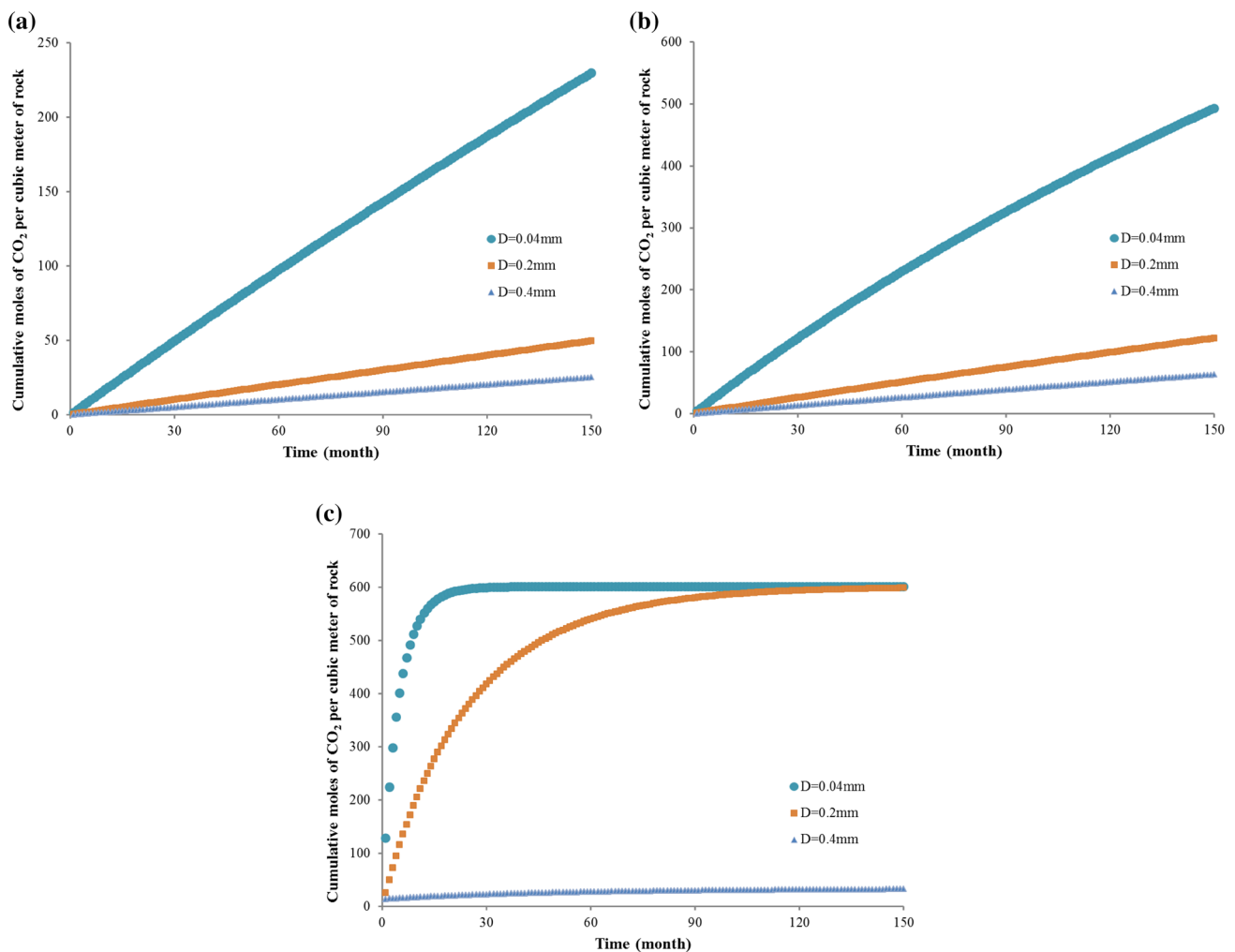


Fig. 11 Cumulative moles of CO₂ per cubic meter of **a** sodium feldspar, **b** potash feldspar, and **c** calcium feldspar for different particle sizes (0.4, 0.2, and 0.04 mm) and same porosity (40%)

Effect of iteration length

The computation method used here involves solving a set of equations iteratively. The dissolution volume in each iteration step (loop) is directly related to the iteration length and the disjoining pressure is updated to use in the calculations in the next step. Therefore, the iteration length employed in the calculation could have an effect on the results obtained for the cumulative amounts of CO₂ sequestered via pressure solution and this possibility should be investigated. In Fig. 12, the results calculated for calcium feldspar using three different iteration lengths (1 day, 1 week, and 1 month) are illustrated and compared.

The final amounts of CO₂ sequestered after 150 months in Fig. 12 are 1294.1, 1294.5, and 1296.9 mol (per cubic meter of calcium feldspar) when iteration lengths of 1 day, 1 week, and 1 month are used, respectively. The differences between these results are insignificant. As can be seen, the

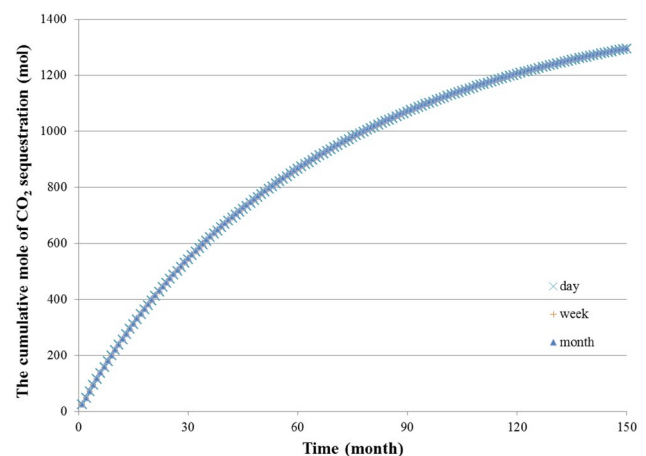


Fig. 12 Cumulative numbers of moles of CO₂ sequestered by pressure solution per cubic meter of calcium feldspar calculated using iteration lengths of 1 day, 1 week, and 1 month

three curves obtained using different iteration lengths essentially overlap one another completely. Therefore, the effect of iteration length on the calculation results presented here can be ignored.

Scope and limitations

It is to be noted that the three principal stresses are assumed to be the same in this article to simplify the calculations. In reality, the three principal stresses will be different, and therefore, differential dissolution rates will be encountered. However, the assumption (that the principal stresses are the same) is acceptable in the contrastive analysis made here as the aim is to demonstrate the effect that pressure solution has on CO₂ sequestration. Of course, if the model was to be applied to evaluate pressure solution and CO₂ mineralization sequestration in a specific stratigraphic environment (especially one subject to tectonic stress), three different principal stresses should be adopted. Moreover, such an improved geometrical model for pressure solution could be used in the field of sedimentology to help explain oriented mineral distribution. As the compressibility modulus of the matrix in a reservoir is much larger than that of the pore fluid, the mechanical deformation of the RVE in the reservoir matrix is ignored in our iterative computations.

Conclusions

CO₂ sequestration in deep saline aquifers is considered to be a feasible and effective way of trapping anthropogenic CO₂. In particular, CO₂-EWR offers certain advantages over traditional carbon capture and storage methods by improving the economic viability of the CO₂ sequestration process and advancing the security and efficiency of CO₂ trapping in deep saline aquifers. Mineral trapping is the most effective way of achieving long-term storage of the CO₂ injected into saline aquifers. In this article, mineral trapping as a chemo-mechanical coupling process is investigated by means of experiment and theoretical model.

As the results of seepage-creep tests performed on sandstone specimens using a flow-through of CO₂-NaCl solution, the influence of pore pressure on the chemo-mechanical mechanism is concluded in terms of creep deformation, pore size distribution, and carbon fixation as the following findings: (1) strain is increased when the pore pressure decreases; (2) pore space and pore pressure are positively correlated; and (3) the lower the pore pressure the specimen is subjected to, the greater the amount of carbon trapped as a solid product in the sandstone specimens.

On the basis of the results observed, the chemo-mechanical coupling mechanism involved in mineral trapping in the rock matrix was quantitatively described using a geometrical

chemo-mechanical coupling model for pressure solution. The model takes into account dissolution in three dimensions according to the three principal stresses. In the model, the evolution of the stress and course of the dissolution are coupled via the area of the contact face (A_c) and rate of change of dissolution volume of the mineral particles (\dot{V}_d). In addition, this chemo-mechanical coupling model could be embedded into numerical simulation of thermo-hydro-chemo-mechanical coupling process in CO₂ sequestration.

The main factors influencing the efficiency of CO₂ mineral trapping in deep saline aquifers (mineral type, temperature, porosity, pore pressure, and particle size) were then investigated using the model to perform numerical calculations. In this way, the cumulative amounts of CO₂ sequestered via pressure solution per cubic meter of sodium, potash, and calcium feldspar could be compared at different temperatures, pore pressures, particle diameters, and porosities. The results show that the amount of CO₂ sequestered via pressure solution can be increased if high geotherm, low pore pressures, and minerals with large porosities and fine particles are taken advantage of.

The results of the analysis imply that the time taken to realize a given CO₂ sequestration target via pressure solution can be shortened if the pore pressure is reduced. This means that mineral trapping can be enhanced if CO₂-EWR is adopted (as this exploits the saline solution in the aquifers and thus releases pore pressure). Apart from this effect, the geothermic gradient, mineral type, particle size, and porosity are the key factors influencing CO₂ mineral trapping via pressure solution. Furthermore, these factors could be used to devise an evaluation index for judging the potential efficiency of the mineralization sequestration process, as well as active management for mineral trapping in CO₂-EWR.

Acknowledgements The authors gratefully acknowledge support by National Natural Science Foundation of China for innovation research groups (Grant no. 51621006) and National Natural Science Foundation of China (General Program Grant nos. 51879261 and 41572296).

References

- Aagaard P, Oelkers EH, Schott J (2004) Glauconite dissolution kinetics and application to CO₂ storage in the subsurface//*Geochimica et Cosmochimica Acta*. Pergamon-Elsevier Science Ltd 68(11):A143–A143
- Ague JJ, Brimhall GH (1989) Geochemical modeling of steady state fluid flow and chemical reaction during supergene enrichment of porphyry copper deposits. *Econ Geol* 84(3):506–528
- Aines RD, Wolery TJ, Bourcier WL, Wolfe T, Hausmann C (2011) Fresh water generation from aquifer-pressured carbon storage: feasibility of treating saline formation waters. *Energy Procedia* 4:2269–2276
- Bachu S (2016) Identification of oil reservoirs suitable for CO₂-EOR and CO₂ storage (CCUS) using reserves databases, with application to Alberta, Canada. *Int J Greenhouse Gas Control* 44:152–165

- Bachu S, Adams JJ (2003) Sequestration of CO₂ in geological media in response to climate change: capacity of deep saline aquifers to sequester CO₂ in solution. *Energy Convers Manage* 44(20):3151–3175
- Birkholzer JT, Zhou Q, Tsang CF (2009) Large-scale impact of CO₂ storage in deep saline aquifers: a sensitivity study on pressure response in stratified systems. *Int J Greenhouse Gas Control* 3(2):181–194
- Birkholzer JT, Cihan A, Zhou Q (2012) Impact-driven pressure management via targeted brine extraction—conceptual studies of CO₂ storage in saline formations. *Int J Greenhouse Gas Control* 7:168–180
- Bond AE, Brusky I, Chittenden N et al (2016) Development of approaches for modelling coupled thermal–hydraulic–mechanical–chemical processes in single granite fracture experiments. *Environ Earth Sci* 75(19):1313
- Buscheck TA, Sun Y, Chen M et al (2012) Active CO₂ reservoir management for carbon storage: analysis of operational strategies to relieve pressure buildup and improve injectivity. *Int J Greenhouse Gas Control* 6:230–245
- Buscheck TA, Bielicki JM, White JA et al (2017) Managing geologic CO₂ storage with pre-injection brine production in tandem reservoirs. *Energy Procedia* 114:4757–4764
- Carroll SA, Knauss KG (2005) Dependence of labradorite dissolution kinetics on CO₂(aq), Al(aq), and temperature. *Chem Geol* 217:213–225
- Coussy O (2004) *Poromechanics*. Wiley, Chichester
- Davidson CL, Dooley JJ, Dahowski RT (2009) Assessing the impacts of future demand for saline groundwater on commercial deployment of CCS in the United States. *Energy Procedia* 1(1):1949–1956
- De Silva GPD, Ranjith PG, Perera MSA (2015) Geochemical aspects of CO₂ sequestration in deep saline aquifers: a review. *Fuel* 155:128–143
- Gérard F, Xu T, Brimhall G, Pruess K (1997) Modeling reactive chemical transport problems with the codes EQ3/6 and TRANQUI: Lawrence Berkeley Laboratory Report. California, Berkeley
- Ghafoori M, Tabatabaei-Nejad SA, Khodapanah E (2017) Modeling rock–fluid interactions due to CO₂ injection into sandstone and carbonate aquifer considering salt precipitation and chemical reactions. *J Nat Gas Sci Eng* 37:523–538
- Gunter WD, Bachu S, Benson S (2004) The role of hydrogeological and geochemical trapping in sedimentary basins for secure geological storage of carbon dioxide. *Geol Soc Lond Spec Publ* 233(1):129–145
- Hangx SJT, Spiers CJ (2009) Reaction of plagioclase feldspars with CO₂ under hydrothermal conditions. *Chem Geol* 265:88–98
- Heidug WK (1995) Intergranular solid–fluid phase transformations under stress: the effect of surface forces. *J Geophys Res Solid Earth* 100(B4):5391–5940
- Hunter K, Bielicki JM, Middleton R et al (2017) Integrated CO₂ storage and brine extraction. *Energy Procedia* 114:6331–6336
- Jiang Q, Su G, Feng XT, Chen G, Zhang MZ, Liu C (2019) Excavation optimization and stability analysis for large underground caverns under high geostress: a case study of the Chinese Laxiwa project. *Rock Mech Rock Eng* 52(3):895–915
- Kobos PH, Cappelle MA, Krumbhansl JL et al (2011) Combining power plant water needs and carbon dioxide storage using saline formations: implications for carbon dioxide and water management policies. *Int J Greenhouse Gas Control* 5(4):899–910
- Labus K, Bujok P, Klempa M et al (2016) Preliminary geochemical modeling of water–rock–gas interactions controlling CO₂ storage in the Badenian Aquifer within Czech Part of Vienna Basin. *Environ Earth Sci* 75(14):1086
- Lemieux JM (2011) Review: the potential impact of underground geological storage of carbon dioxide in deep saline aquifers on shallow groundwater resources. *Hydrogeol J* 19:757–778
- Liteanu E, Niemeijer A, Spiers CJ, Peach CJ, Bresser JHP (2012) The effect of CO₂ on creep of wet calcite aggregates. *J Geophys Res Solid Earth* 117:B03211. <https://doi.org/10.1029/2011JB008789>
- Liu J, Sheng J, Polak A et al (2006) A fully-coupled hydrological–mechanical–chemical model for fracture sealing and preferential opening. *Int J Rock Mech Min Sci* 43(1):23–36
- Myrntinen A, Becker V, Nowak M et al (2012) Analyses of pre-injection reservoir data for stable carbon isotope trend predictions in CO₂ monitoring: preparing for CO₂ injection. *Environ Earth Sci* 67(2):473–479
- Niu Z, Li Q, Wei X et al (2017) Numerical investigation of slippage characteristics of normal and reverse faults under fluid injection and production. *Environ Earth Sci* 76(14):502
- Palandri JL, Rosenbauer RJ, Kharaka YK (2005) Ferric iron in sediments as a novel CO₂ mineral trap: CO₂–SO₂ reaction with hematite. *Appl Geochem* 20(11):2038–2048
- Pietruszczak S, Lydzba D, Shao JF (2006) Modelling of deformation response and chemo-mechanical coupling in chalk. *Int J Numer Anal Meth Geomech* 30(10):997–1018
- Pokrovsky OS, Golubev SV, Schott J et al (2009) Calcite, dolomite and magnesite dissolution kinetics in aqueous solutions at acid to circumneutral pH, 25–150 °C and 1–55 atm pCO₂: new constraints on CO₂ sequestration in sedimentary basins. *Chem Geol* 265(1):20–32
- Randolph JB, Saar MO (2011) Coupling carbon dioxide sequestration with geothermal energy capture in naturally permeable, porous geologic formations: implications for CO₂ sequestration [J]. *Energy Procedia* 4:2206–2213
- Regnault O, Lagneau V, Catalette H et al (2005) Experimental study of pure mineral phases/supercritical CO₂ reactivity. Implications for geological CO₂ sequestration. *CR Geosci* 337:1331–1339
- Stephenson LP, Plumley WJ, Palciauskas VV (1992) A model for sandstone compaction by grain interpenetration. *J Sediment Res* 62(1):11–22
- Taron J, Elsworth D (2010) Coupled mechanical and chemical processes in engineered geothermal reservoirs with dynamic permeability. *Int J Rock Mech Min Sci* 47(8):1339–1348
- Yasuhara H, Kinoshita N, Ohfuji H et al (2011) Temporal alteration of fracture permeability in granite under hydrothermal conditions and its interpretation by coupled chemo-mechanical model. *Appl Geochem* 26(12):2074–2088

Publisher's Note Springer Nature remains neutral with regard to jurisdictional claims in published maps and institutional affiliations.